Advanced Composite Materials
Publication details, including instructions for authors and subscription information:
http://www.tandfonline.com/loi/tacm20

Transverse cracking in CFRP cross-ply laminates with interlaminar resin layers

Shinji Ogihara [a] , Nobuo Takeda [b] & Akira Kobayashi [c]

[a] Department of Mechanical Engineering, Science University of Tokyo, 2641 Yamasaki, Noda, Chiba 278-8510, Japan

[b] Center for Collaborative Research (CCR), The University of Tokyo, 4-6-1 Komaba, Meguro-ku, Tokyo 153-8904, Japan

[c] Department of Mechanical Engineering, Science University of Tokyo, 2641 Yamasaki, Noda, Chiba 278-8510, Japan

Version of record first published: 02 Apr 2012.

To cite this article: Shinji Ogihara , Nobuo Takeda & Akira Kobayashi (1998): Transverse cracking in CFRP cross-ply laminates with interlaminar resin layers, Advanced Composite Materials, 7:4, 347-363

To link to this article: http://dx.doi.org/10.1163/156855198X00246

Adv. Composite Mater., Vol. 7, No. 4, pp. 347–363 (1998)

Transverse cracking in CFRP cross-ply laminates with interlaminar resin layers

SHINJI OGIHARA [1,*], NOBUO TAKEDA [2] and AKIRA KOBAYASHI [1]

[1] *Department of Mechanical Engineering, Science University of Tokyo, 2641 Yamasaki, Noda, Chiba 278-8510, Japan*

[2] *Center for Collaborative Research (CCR), The University of Tokyo, 4-6-1 Komaba, Meguro-ku, Tokyo 153-8904, Japan*

Received 10 February 1998; accepted 22 July 1998

Abstract—In recent years, interlaminar-toughened laminates have been developed in which resin rich layers are placed in interlaminar regions in order to enhance the interlaminar fracture toughness of CFRP laminates. In the present study, a predictive method is developed for transverse cracking in CFRP cross-ply laminates with interlaminar resin layers at 0/90° interfaces under static tensile loading. The analysis is based on a two-dimensional approximate elastic analysis considering the interlaminar resin layers and thermal residual stresses. To predict transverse cracking, both energy and stress criteria are used. The change in thermoelastic properties of a laminate due to transverse cracking is also predicted. To investigate the validity of the analysis, loading–unloading tests are performed to obtain Young's modulus reduction as a function of the transverse crack density. The predictions of transverse crack density as a function of the laminate strain are compared with our previous experimental results. A good agreement is obtained which implies the validity of the present analysis.

Keywords: CFRP; composite material; cross-ply laminate; energy release rate; interlaminar resin layers; interlaminar-toughened laminate; thermal residual stress; transverse cracks; Young's modulus.

1. INTRODUCTION

In many applications of fiber reinforced plastics, fibers are aligned in more than one direction to provide high load-bearing capability. Among these composite laminates, cross-ply laminates have been extensively studied because this is a basic laminate configuration. The failure process of cross-ply laminates under static tensile loading is known to involve a sequential accumulation of damage in the form of matrix-dominated cracking [1]. One type of damage comprises multiple

*To whom correspondence should be addressed. E-mail: ogihara@rs.noda.sut.ac.jp

transverse cracks running parallel to fibers in 90° plies. A second type of damage is delamination.

Transverse cracks in off-axis plies usually occur at a stress which is much lower than the laminate strength. As the laminate stress increases, the number of transverse cracks increases. To establish damage tolerance design of laminated composites, proper methodology to predict transverse crack behavior has to be introduced. That is, a predictive method of transverse crack density as a function of the laminate stress needs to be developed.

From this point of view, many investigations, which consist of experimental observation of onset and multiplication of transverse cracks and its modeling, have been conducted on cross-ply composite laminates as a basis for analyzing laminates with arbitrary laminate configurations.

Bailey *et al.* [2] studied the relation between transverse crack spacing and applied laminate stress using shear-lag analysis. They used the stress criterion which assumes that a transverse crack occurs when the maximum 90° ply stress reaches a critical value. They also showed experimentally that the transverse crack onset strain (first cracking strain) increases with decreasing 90° ply thickness. This phenomenon was called the constraint effect and cannot be explained by the stress criterion. They explained the constraint effect by using the energy balance before and after transverse cracking. Though this concept does not consider the crack propagation in the 90° ply, it can explain the dependence of first cracking strain on the 90° ply thickness. This concept is called the energy criterion.

Predictions of the transverse crack density were also conducted by Laws and Dvorak [3], Han *et al.* [4] (a combination of the shear-lag analysis and the energy criterion), Fukunaga *et al.* [5], Lee and Daniel [6] (a combination of the shear-lag analysis and the strength criterion), Nairn [7] (a combination of the variational stress analysis and the energy criterion), Peters *et al.* [8] and Takeda and Ogihara [9–11] by considering the statistical characteristics of 90° ply strength.

In recent years, interlaminar-toughened laminates have been developed in which resin-rich layers are placed in interlaminar regions in order to enhance the interlaminar fracture toughness of CFRP laminates. Increase in interlaminar fracture toughness by introducing interlaminar resin layers is reported [12–16]. However, transverse cracks will occur in interlaminar-toughened laminates in off-axis plies, because intralaminar fracture toughness is not improved.

The authors [17] have analyzed the stress and displacement fields in an interlaminar toughened CFRP cross-ply laminate with transverse cracks. The analysis was based on the two-dimensional analysis conducted by McCartney [18]. The prediction of displacement fields in a cracked cross-ply laminate was successfully compared with our experimental results using the *in-situ* SEM/micro-line methods, which implies the validity of the analysis [19].

In the present study, transverse crack density was predicted by using both energy and stress criteria based on the analysis. Furthermore, change in thermoelastic properties of the cracked laminates with transverse crack density was predicted. The

prediction of transverse crack density was compared with our previous experimental results [20]. Loading–unloading tests were also performed to obtain Young's modulus reduction as a function of transverse crack density and to compare with the prediction. A good agreement was obtained, which implies the validity of the present analysis. The analysis will provide a basis for the optimal design of this type of laminated composites.

2. ANALYSIS

2.1. Prediction of transverse cracking

The authors [17] analyzed the stress and displacement fields in interlaminar toughened cross-ply laminates with transverse cracks as shown in Fig. 1. The analysis is based on two-dimensional approximate elastic analysis for a cross-ply laminates without interlaminar resin layers conducted by McCartney [18].

A set of rectangular Cartesian co-ordinates (x, y, z) is selected as shown in Fig. 1. The laminate is subjected to a tensile stress, σ, in the y-direction. It is assumed that a parallel array of equally spaced (crack spacing is $2L$) transverse cracks that run through the thickness and width of the 90° ply occurs. The transverse crack tips stop at the 90°/interlaminar resin layer interface. The thicknesses of the outer 0° ply, interlaminar resin layer and inner 90° ply are b, t and $2a$, respectively. The laminate thickness is denoted by $2h$, where $h = b + t + a$. A generalized plane strain condition is assumed and the stress and displacement fields are expressed as functions of x and y [17].

In the present study, a prediction of the transverse crack density as a function of the applied laminate stress (or strain) is conducted by using the results of the analysis [17]. Both the stress and energy criteria are considered.

In the stress criterion, it is assumed that a transverse crack occurs when the normal stress in the y-direction in 90° ply reaches a critical value. The normal stress in the

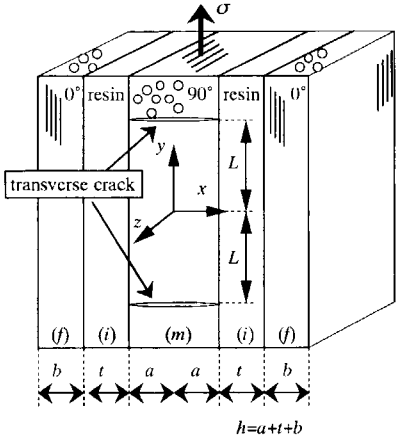

Figure 1. A model of interlaminar-toughened cross-ply laminate containing transverse cracks in 90° ply.

y-direction in 90° ply reaches its maximum value midway between the transverse cracks, that is, $y = 0$. When the transverse crack spacing is $2L$, the maximum normal stress in the y-direction in the 90° ply is

$$\sigma^{m}_{yy,\max} = -\frac{b}{a}P(\sigma, 2L) + \sigma_m, \tag{1}$$

where σ_m is 90° ply normal stress in the y-direction in the damage-free laminate and P the change in stress with transverse cracking. The parameter P is a function of the laminate stress (σ) and transverse crack spacing ($2L$) and is shown in the Appendix. Assuming that the critical value is σ_B, the transverse crack spacing will be L when the value of the left hand of equation (1) reaches σ_B. Then, the relation between the transverse crack spacing, L, and the laminate stress, σ, is given by the following equation.

$$\sigma_B = -\frac{b}{a}P(\sigma, 2L) + \sigma_m. \tag{2}$$

In the energy criterion, it is assumed that a transverse crack occurs when the energy release rate associated with transverse cracking reaches a critical value. The energy release rate associated with transverse cracking can be derived using the previous analysis [17]. Assuming that transverse cracks occur at a constant load, the energy release rate, G_t, associated with transverse crack formation midway between the transverse cracks whose spacing is $2L$ is expressed as

$$G_t = \frac{1}{a}\left(\sigma - E_A\alpha_A\Delta T\right)^2 hL\left(\frac{1}{E_c(L)} - \frac{1}{E_c(2L)}\right). \tag{3}$$

Then, the laminate stress when the transverse crack spacing becomes L from $2L$ is shown to be

$$\sigma = \sqrt{\frac{aG_{tc}}{hL}\left(\frac{1}{E_c(L)} - \frac{1}{E_c(2L)}\right)^{-1}} + E_A\alpha_A\Delta T, \tag{4}$$

where E_A and α_A are the axial Young's modulus and the axial thermal expansion coefficient of the damage-free laminate, respectively, $E_c(L)$ and $E_c(2L)$ axial Young's modulus of the laminates with transverse cracks whose spacing is L and $2L$, respectively. $\Delta T = T - T_0$, where T is the test temperature, and T_0 is the stress-free temperature. The parameters are obtained in the analysis [17] and are shown in the Appendix.

2.2. *Prediction of change in thermoelastic properties due to transverse cracking*

Using the results of the analysis, change in thermoelastic properties of laminates due to transverse cracking can be derived. Let ε_c be the longitudinal strain of the laminate with transverse cracks; then the following relation is obtained.

$$\bar{v}_f(L) = L\varepsilon_c, \tag{5}$$

$$\bar{v}_f(y) = \frac{1}{b}\int_{a+t}^{h} v_f(x, y)\,\mathrm{d}x, \tag{6}$$

where $v_f(x, y)$ is the displacement of the 0° ply in the y-direction. On substituting the results obtained by the analysis [17] into (5), the following relation is obtained.

$$\varepsilon_c = \varepsilon + \frac{a}{L}\frac{\sigma_m}{E'^f_A}\Phi. \tag{7}$$

Parameters in the equation are obtained and also shown in the Appendix. Making some manipulations on (7), the following stress–strain relation for the laminates with transverse cracks is obtained.

$$\varepsilon_c = \frac{\sigma}{E_c} + \alpha_c \Delta T, \tag{8}$$

where E_c and α_c are the longitudinal Young's modulus and longitudinal thermal expansion coefficient of the laminate with transverse cracks, respectively, and are given in the Appendix. For the transverse strain, ε^*, of the laminate with transverse cracks,

$$\varepsilon^* = -\frac{\nu_c}{E_c}\sigma + \alpha_c^* \Delta T, \tag{9}$$

where ν_c and α_c^* are Poisson's ratio and transverse thermal expansion coefficient of the laminate with transverse cracks, respectively, and are also given in the Appendix.

3. EXPERIMENTAL PROCEDURE

3.1. Materials

Two material systems were used. One was interleaved CFRP, T800H/3631-FM300 $(0/90_m/0)$ where $m = 4$, 8 and 12, with epoxy resin (FM300) layers of thickness about 100 μm between the 0° and 90° plies. Another was toughness-improved CFRP, T800H/3900-2 $(0/90_m/0)$ where $m = 4$, 8 and 12, with selectively toughened interlaminar layers of thickness about 30 μm at all ply interfaces. The interlaminar layers contain tough and fine polyamide particles dispersed in epoxy matrix [15, 16].

T800H is a high strength carbon fiber. The 3631 is a modified epoxy system with improved toughness compared with conventional TGDDM/DDS epoxy resin. The base resin of 3900-2 is similar to 3631. The average thickness of each ply was 0.135 mm for T800H/3631-FM300 and 0.190 mm for T800H/3900-2. The fiber volume fractions were 43–47% for T800H/3631-FM300 and 54–55% for T800H/3900-2. The low fiber volume fraction for T800H/3631-FM300 is due to the thick FM300 resin film.

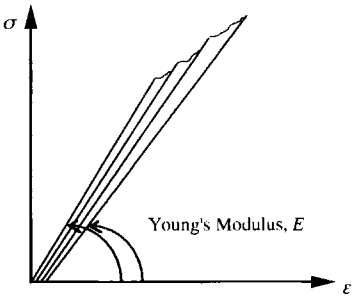

Figure 2. Schematic illustration of loading–unloading test.

3.2. Tensile test — measurement of transverse crack density

Tensile tests were performed to obtain the transverse crack density as a function of the laminate strain. To investigate the temperature effects, the tests were conducted both at room temperature (R.T.) and at 80°C. During the tensile tests, the polished edge surface of a specimen was replicated on cellulose acetate film with methyl acetate as a solvent. The most important advantage of this technique is that the damage state of a large area at each load level can be preserved after a test. The transverse crack density was defined as the number of transverse cracks per unit specimen length.

3.3. Loading–unloading test — measurement of Young's modulus reduction

Loading–unloading tests were also performed to obtain the Young's modulus reduction as a function of the transverse crack density. The loading–unloading procedure cycles were repeated several times with the continuous recording of the stress–strain curves. To investigate the temperature effects, the tests were conducted both at R.T. and at 80°C. The specimen edge was replicated at each perfectly unloaded point. The Young's modulus reduction as a function of the transverse crack density was obtained based on the combination of the replica observation and the measurement of the stress–strain curves. Figure 2 shows a schematic illustration of the loading–unloading test.

4. RESULTS AND DISCUSSION

4.1. Prediction of transverse crack density

During the tensile loading, the microscopic damage observed was transverse cracks in the 90° ply in both material systems [20]. The transverse cracks were always observed in the form that they ran through the thickness and width of the 90° ply. It was also observed that a new transverse crack occurs at almost the midpoint between the existing two transverse cracks. The micro-optical observation from both specimen edges and observation with a scanning acoustic microscope showed

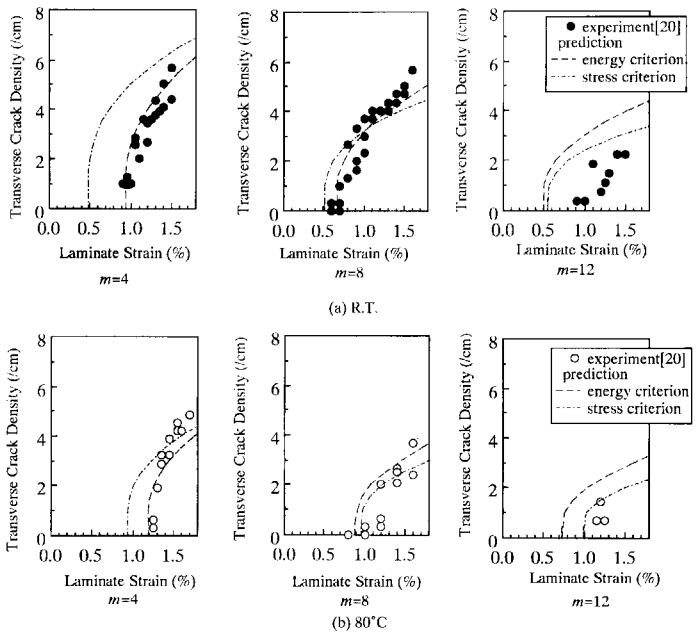

Figure 3. Transverse crack density as a function of applied laminate strain in T800H/3631-FM300 $(0/90_m/0)$. (a) R.T. (b) 80°C. Comparison between experimental results [20] and analytical predictions.

that the transverse crack spanned the entire specimen width. The transverse crack surface is normal to the loading direction. In these material systems, delamination at the 0/90 interface from the transverse crack tip was not observed. Since the authors observed delamination in T800H/3631 $(0/90_m/0)$ ($m = 4$, 8 and 12) laminates without interlaminar resin layers [10], it is found that the enhancement of interlaminar fracture toughness due to the introduction of interlaminar resin layers is achieved.

Figures 3 and 4 show experimental results for the transverse crack density as a function of the applied laminate strain in T800H/3631-FM300 and T800H/3900-2, respectively.

In both material systems, the first cracking strains for $m = 4$ and 12 are larger than that for $m = 8$ at the same temperature. The transverse crack density decreases with increasing m (90° ply thickness) in this temperature range. The first cracking strain is larger at 80°C than that at R.T. for the same m. This is because the tensile thermal residual stress in 90° ply decreases and the 90° ply failure strain increases as temperature increases.

Figure 5 shows plots of the predictions of transverse crack density as a function of the applied laminate strain by using the stress and energy criteria for T800H/3631-FM300 at R.T. Material properties used in this prediction is shown in Table 1. The critical values are for the stress criterion, $\sigma_B = 90$ MPa and for the energy criterion, $G_{Ic} = 700$ J/m^2.

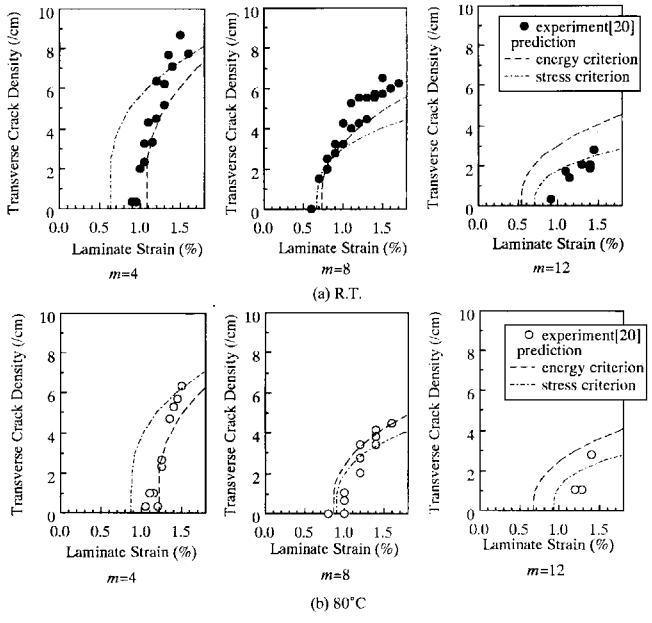

Figure 4. Transverse crack density as a function of applied laminate strain in T800H/3900-2 $(0/90_m/0)$. (a) R.T. (b) 80°C. Comparison between experimental results [20] and analytical predictions.

Table 1.
Material properties used in the analysis

Composite	T800H/3631	T800H/3900-2	Resin	FM300	Polyamide particle-dispersed layer
E_A (GPa) (R.T.)	152.2	130.4	E^i (GPa) (R.T.)	2.45	2.50
(80°C)	144.2	126.4	(80°C)	1.23	1.87
E_T (GPa) (R.T.)	9.57	7.96	μ^i (GPa) (R.T.)	0.88	0.91
(80°C)	8.09	7.30	(80°C)	0.44	0.68
μ_A (GPa) (R.T.)	4.50	4.50	ν^i	0.38	0.38
(80°C)	4.26	3.80			
μ_T (GPa) (R.T.)	3.21	2.67	α^i ($\times 10^{-6}$)	60.0	60.0
(80°C)	2.75	2.45			
ν_A	0.349	0.349			
ν_T	0.490	0.490			
α_A ($\times 10^{-6}$)	0.100	− 1.73			
α_T ($\times 10^{-6}$)	35.5	34.7			
σ_B (MPa) (R.T.)	90	90			
(80°C)	100	90			
G_{Ic} (J/m^2) (R.T.)	700	500			
(80°C)	1000	600			

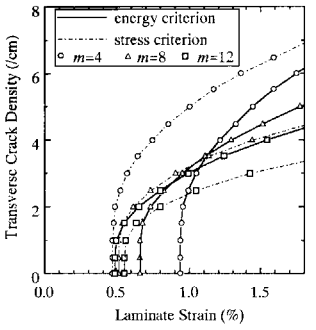

Figure 5. Predictions of transverse crack density as a function of laminate strain in T800H/3631-FM300 ($0/90_m/0$) cross-ply laminates. Comparison between the energy and stress criteria for various 90° ply thicknesses.

All the predictions of the transverse crack density are increasing functions of the laminate strain and the derivative decreases as the strain increases. When the critical values are set larger, the predicted first cracking strain gets larger and smaller transverse crack density is predicted for the same laminate strain (this is not shown in the figure). As shown in Fig. 5, the first cracking strain increases as m increases in the stress criterion. This corresponds to the decreasing tensile thermal residual strain in the 90° ply with increasing m. In the energy criterion, the first cracking strain is smaller for larger m. This is due to the fact that the energy release rate is larger for larger m. For a laminate configuration, two prediction curves exist. Transverse cracks can be considered to occur when both the stress and energy criteria are satisfied. If this is true, it should be reasonable to regard the prediction that gives smaller transverse crack density as the prediction of the present analysis.

Considering the discussion above, comparisons between the experimental results and the analytical predictions are conducted as shown in Figs 3 and 4 assuming the critical values. Material properties used in the analysis are listed in Table 1. The values for T800H/3631 and T800H/3900-2 are taken from [9] and [20], respectively, and those for FM300 at R.T. are taken from [12]. The values for FM300 at 80°C are assumed values. Poisson's ratios are assumed to be constant in this temperature range. The curing temperature of the laminates is 180°C for both material systems.

The critical values used are $\sigma_B = 90$ MPa (R.T.), 100 MPa (80°C), $G_{Ic} = 700$ J/m^2 (R.T.), 1000 J/m^2 (80°C) for T800H/3631-FM300 and $\sigma_B = 90$ MPa (R.T.), 90 MPa (80°C), $G_{Ic} = 500$ J/m^2 (R.T.), 600 J/m^2 (80°C) for T800H/3900-2. In this temperature range, the change in the critical value for the stress criterion is small. The critical value for the energy criterion increases as temperature increases due to the increase in toughness of the matrix material.

In Figs 3 and 4, a reasonable agreement between the experimental results and analytical prediction is obtained if the criterion which gives smaller transverse crack density is selected. Clearly, it cannot be explained that the first cracking strain is lower for $m = 8$ than that for $m = 4$ by only the stress criterion. It cannot be

explained that the first cracking strain is higher for $m = 12$ than that for $m = 8$ by only the energy criterion. By using both criteria, it will be possible to predict transverse cracking behavior in the laminates with more extensive range of laminate configuration. The analysis will be a useful tool for the optimal design of this type of composite laminates.

4.2. *Change in thermoelastic properties of the laminate*

Figures 6 and 7 show the comparison of experimental data and analytical predictions of Young's modulus reduction as a function of the transverse crack density for T800H/3631-FM300 and T800H/3900-2, respectively. Young's modulus is normalized with the value of the damage-free laminate. A reasonable agreement is obtained for both material systems in this temperature range, which implies the validity of this analysis.

Figure 8 shows analytical results for change in longitudinal thermal expansion coefficient as a function of transverse crack density for T800H/3631-FM300. Lim and Hong [21] conducted the shear-lag analysis to predict the change in thermal expansion coefficient with transverse crack density and compared with FEM analysis. The results they obtained showed that the normalized thermal

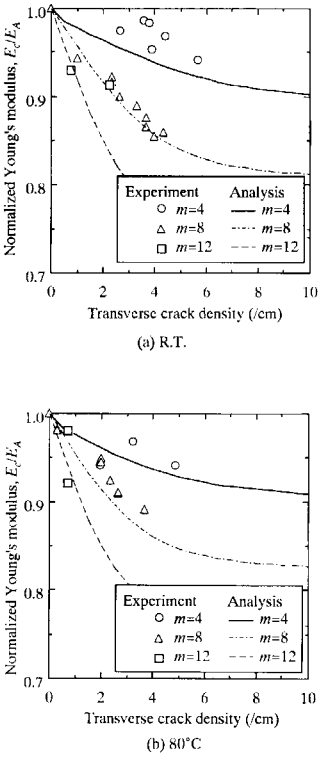

Figure 6. Normalized Young's modulus as a function of transverse crack density in T800H/3631-FM300 cross-ply laminates $(0/90_m/0)$. (a) R.T. (b) 80 °C.

expansion coefficients decreases as transverse crack density increases and that the normalized thermal expansion coefficients are smaller for the laminates with thicker 90° ply at the same transverse crack density. In this analysis, a similar tendency to Lim and Hong's results [21] is obtained.

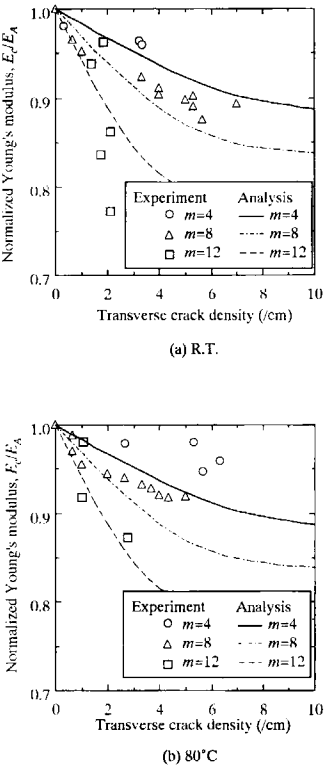

Figure 7. Normalized Young's modulus as a function of transverse crack density in T800H/3900-2 cross-ply laminates $(0/90_m/0)$. (a) R.T. (b) 80°C.

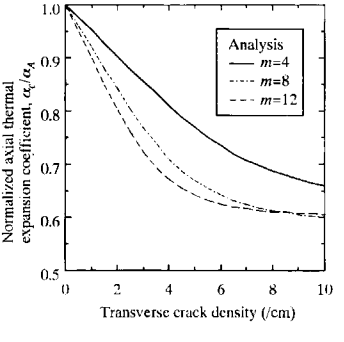

Figure 8. Normalized axial thermal expansion coefficient as a function of transverse crack density in T800H/3631-FM300 cross-ply laminates $(0/90_m/0)$.

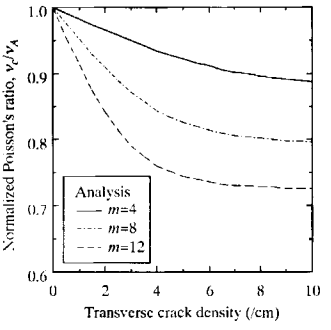

Figure 9. Normalized Poisson's ratio as a function of transverse crack density in T800H/3631-FM300 cross-ply laminates $(0/90_m/0)$.

Figure 9 shows analytical results for change in Poisson's ratio as a function of the transverse crack density for T800H/3631-FM300. As transverse crack density increases, the normalized Poisson's ratio decreases. The normalized Poisson's ratio is smaller for the laminates with thicker 90° ply. These results are consistent with the analytical results obtained by McCartney [18], which implies the validity of the present analysis.

5. CONCLUSIONS

A predictive method was developed for transverse cracking in cross-ply laminates with interlaminar resin layers. The change in thermoelastic properties of the laminate due to transverse cracking was also predicted. The analysis was based on the two-dimensional approximate elastic analysis considering the interlaminar resin layers and thermal residual stresses. The analytical results were successfully compared with the experimental results. The validity of the energy criterion and strength criterion was discussed. It was found that the criterion which gives smaller transverse crack density should be selected. The analysis presented in the present paper will be a basis for the optimal design of laminated composites with interlaminar resin layers.

REFERENCES

1. J. E. Masters and K. L. Reifsnider, An investigation of cumulative damage development in quasi-isotropic graphite/epoxy laminates, Damage in composite materials, in: *ASTM STP 775*, K. L. Reifsnider (Ed.), pp. 40–62. American Society for Testing and Materials, Philadelphia (1982).
2. J. E. Bailey, P. T. Curtis and A. Parvizi, On the transverse cracking and longitudinal splitting behavior of glass and carbon fiber reinforced epoxy cross ply laminates and the effect of Poisson and thermally generated strain, *Proc. Roy. Soc. Lond. A* **366**, 599–623 (1979).
3. N. Laws and G. J. Dvorak, Progressive transverse cracking in composite laminates, *J. Compos. Mater.* **22**, 900–916 (1988).

4. Y. M. Han, H. T. Hahn and R. B. Croman, A simplified analysis of transverse ply cracking in cross-ply laminates, *Compos. Sci. Technol.* **31**, 165–177 (1988).
5. H. Fukunaga, T.-W. Chou, P. W. M. Peters and K. Schulte, Probabilistic failure strength analyses of graphite/epoxy cross-ply laminate, *J. Compos. Mater.* **18**, 339–356 (1984).
6. J.-W. Lee and I. M. Daniel, Progressive transverse cracking of crossply composite laminates, *J. Compos. Mater.* **24**, 1225–1243 (1990).
7. J. A. Nairn, The strain energy release rate of composite microcracking: a variational analysis, *J. Compos. Mater.* **23**, 1106–1129 (1989).
8. P. W. M. Peters, The influence of fiber, matrix and interface on transverse cracking in carbon fiber reinforced plastic cross-ply laminates, in: *ASTM STP 1012*, pp. 103–117 (1989).
9. N. Takeda and S. Ogihara, *In-situ* observation and probabilistic prediction of microscopic failure process in CFRP cross-ply laminates, *Compos. Sci. Technol.* **52**, 189–195 (1994).
10. N. Takeda and S. Ogihara, Initiation and growth of delamination from the tips of transverse cracks in CFRP cross-ply laminates, *Compos. Sci. Technol.* **52**, 309–318 (1994).
11. S. Ogihara and N. Takeda, Interaction between transverse cracks and delamination during damage progress in CFRP cross-ply laminates, *Compos. Sci. Technol.* **54**, 395–404 (1995).
12. E. Altus and O. Ishai, The effect of soft interleaved layers on the combined transverse cracking/delamination mechanisms in composite laminates, *Compos. Sci. Technol.* **39**, 13–27 (1990).
13. A. Askoy and L. A. Carlsson, Interlaminar shear fracture of interleaved graphite/epoxy composites, *Compos. Sci. Technol.* **43**, 55–69 (1992).
14. F. Ozdil and L. A. Carlsson, Plastic zone estimates in mode I interlaminar fracture of interleaved composites, *Engng Fract. Mech.* **41**, 645–658 (1992).
15. N. Odagiri, T. Muraki and K. Tobukuro, Toughness improved high performance torayca prepreg T800H/3900 series, in: *Proc. 33rd Intern. SAMPE Symp.*, pp. 272–283 (1988).
16. N. Odagiri, H. Kishi and T. Nakae, T800H/3900-2 toughened epoxy prepreg system: Toughening concept and mechanism, in: *Proc. Amer. Soc. Composites 6th Technical Conf.*, pp. 43–52 (1991).
17. S. Ogihara, N. Takeda and A. Kobayashi, Analysis of stress and displacement fields in interlaminar-toughened composite laminates with transverse cracks, *Adv. Composite Mater.* 7 (2), 151–168 (1998).
18. L. N. McCartney, Theory of stress transfer in a $0°-90°-0°$ cross-ply laminate containing a parallel array of transverse cracks, *J. Mech. Phys. Solids* **40**, 27–68 (1992).
19. N. Takeda and S. Ogihara, Submitted for publication.
20. S. Ogihara, N. Takeda and A. Kobayashi, Experimental characterization of microscopic failure process under quasi-static tension in interleaved and toughness-improved CFRP cross-ply laminates, *Compos. Sci. Technol.* **57**, 267–275 (1997).
21. S. G. Lim and C. S. Hong, Effect of transverse cracks on the thermomechanical properties of cross-ply laminated composites, *Compos. Sci. Technol.* **34**, 145–162 (1989).

APPENDIX

The authors analyzed the stress and displacement fields in an interlaminar-toughened cross-ply laminate with interlaminar resin layers at 0/90 interfaces [17]. The analysis is based on two-dimensional elastic analyses conducted by McCartney [18] and extended to consider the effects of interlaminar resin layers. In the present paper, the transverse crack density is predicted as a function of applied laminate stress using both the stress and energy criteria. The details of the parameters were described in [17], but are shown in the following for completeness.

P and σ_m in equations (1) and (2) are

$$P = \Lambda\left(q \sinh \frac{pL}{b} \cosh \frac{qL}{b} + p \cosh \frac{pL}{b} \sinh \frac{qL}{b}\right)\frac{a}{b}\sigma_m, \tag{A1}$$

$$\sigma_m = \frac{E'^m_T}{\xi}\left\{\left(1 - \nu_A \nu^m_A\right)\frac{\sigma}{E_A} + \left(\alpha_A + \nu^m_A \alpha_T - \alpha'^m_T\right)\Delta T\right\}, \tag{A2}$$

ε in equation (7) is

$$\varepsilon = \frac{\sigma}{E_A} - \frac{\nu_A}{E_A}\left(\nu^m_A - \nu^f_A \frac{E^f_T}{E^f_A}\right)\frac{ab}{hL}\Phi\sigma_m + \alpha_A \Delta T. \tag{A3}$$

The thermoelastic properties of the cracked laminates are

$$\frac{1}{E_c} = \frac{1}{E_A}\left[1 + \frac{a\Phi E'^m_T}{L\xi}\left\{\frac{1}{E'^f_A} - \frac{\nu_A}{E_A}\left(\nu^m_A - \nu^f_A \frac{E^f_T}{E^f_A}\right)\left(1 - \nu_A \nu^m_A\right)\right\}\right], \tag{A4}$$

$$\alpha_c = \alpha_A + \frac{a\Phi E'^m_T}{L\xi}\left\{\frac{1}{E'^f_A} - \frac{\nu_A}{E_A}\left(\nu^m_A - \nu^f_A \frac{E^f_T}{E^f_A}\right)\right\}\left(\alpha_A + \nu^m_A \alpha_T - \alpha'^m_T\right), \tag{A5}$$

$$\nu_c = \frac{E_c}{E_A}\left[\nu_A - \left(\nu^m_A - \nu^f_A \frac{E^f_T}{E^f_A}\right)\left(1 - \nu_A \nu^m_A\right)\frac{ab\Phi E'^m_T}{hL\xi E_T}\right], \tag{A6}$$

$$\alpha^*_c = \alpha_T + \left(\nu^m_A - \nu^f_A \frac{E^f_T}{E^f_A}\right)\left(\alpha_A + \nu^m_A \alpha_T - \alpha'^m_T\right)\frac{ab\Phi E'^m_T}{hL\xi E_T}, \tag{A7}$$

where

$$\xi = 1 - \left(\nu^m_A - \nu^f_A \frac{E^f_T}{E^f_A}\right)\left(\frac{\nu^m_A}{E_T} - \frac{E'^m_T}{E_A}\nu_A\right)\frac{ab\Phi}{hL}, \tag{A8}$$

$$\Phi = \frac{2\Lambda pq}{p^2 - q^2}\left(\sinh^2 \frac{pL}{b} \cosh^2 \frac{qL}{b} - \cosh^2 \frac{pL}{b} \sinh^2 \frac{qL}{b}\right), \tag{A9}$$

$$\frac{1}{\Lambda} = p \sinh \frac{qL}{b} \cosh \frac{qL}{b} + q \cosh \frac{pL}{b} \sinh \frac{pL}{b}, \tag{A10}$$

$$p = \left[\frac{1}{2}(r + s)\right]^{\frac{1}{2}}, \quad q = \left[\frac{1}{2}|r - s|\right]^{\frac{1}{2}}, \tag{A11}$$

$$r = \frac{G}{2F}, \quad s = \left(\frac{H}{F}\right)^{\frac{1}{2}}, \tag{A12}$$

$$F = \frac{1}{b^4}\left(\frac{b}{t+b}\left[\frac{b^4}{20E'^f_T} + \frac{b^2t(t+b)}{4E'^i} - \frac{ab}{6E'^m_T}\{a-3(h+t)\}\left(\frac{b}{2}+t\right) + \frac{bt^2}{E'^i}\left(\frac{t}{3}+\frac{b}{4}\right)\right] + \frac{t}{t+b}\left[\frac{bt^2(3t+2b)}{24E'^i} - \frac{abt}{12E'^m_T}\{a-3(h+t)\}\right] + \frac{a^2b}{6E'^m_T}\left(-\frac{a}{5}+h+t\right)\right), \tag{A13}$$

$$G = \frac{1}{b^2}\left[\frac{b^2}{t+b}\left\{\frac{b}{3\mu^f_A} + \frac{bv'^f_A}{3E'^f_A} + \left(\frac{1}{\mu^i} - \frac{v'^m_T}{E'^m_T}\right)t - \frac{bv'^m_T}{2E'^m_T}\right\} + \frac{t}{t+b}\left\{\left(\frac{1}{\mu^i} - \frac{v'^m_T}{E'^m_T}\right)\frac{bt}{2} + \frac{v'^i b(t+b)}{2E'^i}\right\} + \frac{ab}{3}\left(\frac{1}{\mu^m_T} - \frac{v'^m_T}{E'^m_T}\right) - \frac{bv'^m_T}{2E'^m_T}\left(h+t-\frac{a}{3}\right)\right], \tag{A14}$$

$$H = b\left(\frac{1}{(t+b)E'^f_A} + \frac{1}{aE'^m_T}\right), \tag{A15}$$

$$E_A = A - \frac{B^2}{C}, \quad E_T = C - \frac{B^2}{A}, \quad v_A = \frac{B}{C}, \tag{A16}$$

$$\alpha_A = (D - v_A E)/E_A, \quad \alpha_T = \left(E - v_A\frac{E_T}{E_A}D\right)/E_T, \tag{A17}$$

$$A = \frac{b\hat{E}^f_A + t\hat{E}^i + a\hat{E}^m_T}{h}, \tag{A18}$$

$$B = \frac{bv^f_A\hat{E}^f_A + tv^i\hat{E}^i + av^m_A\hat{E}^m_T}{h}, \tag{A19}$$

$$C = \frac{b\hat{E}^f_T + t\hat{E}^i + a\hat{E}^m_A}{h}, \tag{A20}$$

$$D = \frac{b\hat{E}^f_A\hat{\alpha}^f_A + t\hat{E}^i\hat{\alpha}^i + a\hat{E}^m_T\hat{\alpha}^m_T}{h}, \tag{A21}$$

$$E = \frac{b\hat{E}^f_T\hat{\alpha}^f_T + t\hat{E}^i\hat{\alpha}^i + a\hat{E}^m_A\hat{\alpha}^m_A}{h}, \tag{A22}$$

$$\frac{1}{\hat{E}_A^f} = \frac{1}{E_A^f}\left\{1 - \left(\nu_A^f\right)^2 \frac{E_T^f}{E_A^f}\right\}, \quad \hat{\alpha}_A^f = \alpha_A^f + \nu_A^f \frac{E_T^f}{E_A^f}\alpha_T^f, \tag{A23}$$

$$\frac{1}{\hat{E}_T^f} = \frac{1}{E_T^f}\left\{1 - \left(\nu_A^f\right)^2 \frac{E_T^f}{E_A^f}\right\}, \quad \hat{\alpha}_T^f = \alpha_T^f + \nu_A^f \alpha_A^f, \tag{A24}$$

$$\frac{1}{\hat{E}^i} = \frac{1 - (\nu^i)^2}{E^i}, \quad \hat{\alpha}^i = \alpha^i\left(1 + \nu^i\right), \tag{A25}$$

$$\frac{1}{\hat{E}_T^m} = \frac{1}{E_T^m}\left\{1 - \left(\nu_A^m\right)^2 \frac{E_T^m}{E_A^m}\right\}, \quad \hat{\alpha}_T^m = \alpha_T^m + \nu_A^m \alpha_A^m, \tag{A26}$$

$$\frac{1}{\hat{E}_A^m} = \frac{1}{E_A^m}\left\{1 - \left(\nu_A^m\right)^2 \frac{E_T^m}{E_A^m}\right\}, \quad \hat{\alpha}_A^m = \alpha_A^m + \nu_A^m \frac{E_T^m}{E_A^m}\alpha_T^m, \tag{A27}$$

$$\begin{aligned} &\frac{1}{E'^f_T} = \frac{1 - \left(\nu_T^f\right)^2}{E_T^f}, \quad \frac{\nu'^f_A}{E'^f_A} = \frac{\nu_A^f\left(1 + \nu_T^f\right)}{E_A^f}, \\ &\frac{1}{E'^f_A} = \frac{1}{E_A^f}\left\{1 - \left(\nu_A^f\right)^2 \frac{E_T^f}{E_A^f}\right\}, \end{aligned} \tag{A28}$$

$$\alpha'^f_T = \left(1 + \nu_T^f\right)\alpha_T^f, \quad \alpha'^f_A = \alpha_A^f + \nu_A^f \frac{E_T^f}{E_A^f}\alpha_T^f, \tag{A29}$$

$$\frac{1}{E'^i} = \frac{1 - \nu^{i2}}{E'^i}, \quad \nu'^i = \frac{\nu^i}{1 - \nu^i}, \tag{A30}$$

$$\alpha'^i = \alpha^i\left(1 + \nu^i\right), \tag{A31}$$

$$\frac{1}{E'^m_T} = \frac{1}{E_T^m}\left\{1 - \left(\nu_A^m\right)^2 \frac{E_T^m}{E_A^m}\right\}, \quad \frac{\nu'^m_T}{E'^m_T} = \frac{1}{E_T^m}\left\{\nu_T^m + \left(\nu_A^m\right)^2 \frac{E_T^m}{E_A^m}\right\}, \tag{A32}$$

$$\alpha'^m_T = \alpha_T^m + \nu_A^m \alpha_A^m. \tag{A33}$$

In the relations $\Delta T = T - T_0$, where T is the test temperature, and T_0 is the stress-free temperature. The parameters E_A, ν_A, μ_A and α_A are axial Young's modulus, Poisson's ratio, shear modulus and thermal expansion coefficient, and E_T, ν_T, μ_T and α_T are the corresponding transverse properties. It should be noted that $E_T = 2\mu_T(1 + \nu_T)$ but $E_A \neq 2\mu_A(1 + \nu_A)$. The thermoelastic constants, which are associated with the 0° ply are denoted by a superscript or subscript f. The corresponding quantities associated with the interlaminar resin layer and the 90°

ply are denoted by a superscript or subscript, i and m, respectively. The symbols f and m were used by McCartney [18] and the symbol i is introduced in the previous paper [17].